Analysis of the Influence of PV Integration on an Unbalanced Grid Voltage Deviation

A. ABAYOMI, AGHA F. NNACHI
Department of Electrical Engineering,
Tshwane University of Technology, eMalahleni,
SOUTH AFRICA

Abstract: - With the increasing utilization of renewable energy sources (RES) to mitigate climate pollution from fossil fuel-based energy production, it is imperative to investigate the influence of integrated Photovoltaic (PV) generation on distribution grid voltage levels and power losses. Voltage stability in dispersed systems with high PV penetration is a major challenge due to solar power dynamic generation. Voltage stability is an important parameter for measuring the level of penetration of PV systems on distribution grids in terms of load capacity. As a result, this study provides analytical voltage stability, which is achieved using a 4.16 kV voltage level on a modified IEEE 13 bus radial distribution system. The network was modeled, simulated, and analyzed based on a snapshot power flow solution. Four simulation scenarios were tested for PV penetration levels on the grid. The collected outcomes demonstrated that the system voltage profile and losses remained within the voltage limit established by international standards with PV penetration. As a result, PV penetration levels greater than 40% of the loading capacity resulted in voltage increases that exceeded the prescribed limits, reverse power flow, and an increase in grid power loss.

Key-Words: - PV generation, losses, PV placement, low-voltage grid, deviation, modeling, InCond MPPT algorithm, dynamic gravity search algorithm, voltage drop, reverse power flow.

Received: April 11, 2024. Revised: August 17, 2024. Accepted: September 17, 2024. Published: October 24, 2024.

1 Introduction

The low-voltage distribution system has undergone an immense rise in the integration of renewable energy sources (RES), driven by global demand for sustainable and clean energy alternatives. Solar photovoltaic (PV) and wind power generation systems are two of the most common RES technologies, as shown in Figure 1, [1]. PV system penetration into the distribution grid is increasing year after year, particularly in densely populated urban regions, where consumers are driven to environmentally benign energy options and lower installation costs. However, as the number of PV generators connected to the distribution network grows, maintaining voltage levels within acceptable limits becomes more difficult due to the grid's original architecture, which failed to account for bidirectional power flows. This is because these PV generators are dependent on fluctuating weather conditions, [2]. It can be integrated into both transmission and distribution networks, including medium- medium and small-scale small-distributed generation systems, [3], [4]. Large-scale Large PV generators, typically three-phase and ranging from an output of 1 to 10 MW, are connected to the power grid through interconnection via connection transformers connected in parallel. These systems are either directly integrated directly into the transmission network or connected to dedicated special distribution substation feeders equipped with voltage and overcurrent protection. Medium-scale Medium-sized PV units, systems with capacities outputs between 10 and 1000 kW and are usually installed in commercial buildings. With the exception of the transformer's rated power, larger units with hundreds of kW are configured similarly to large PV systems, [5], [6]. The 10 kW maximum output small photovoltaic generator is integrated into the home of the energy consumer and is typically single-phase. The most popular type requires no connection transformer at this installation level, [7]. The power grid's PV system penetration was found to be highest in the distribution system, [8]. Small-scale generating and industrial customers will continue to integrate PV into the grid system as a result of government incentives and falling PV panel costs, as PV penetration is believed to provide technical and environmental benefits, [9], [10]. However, high PV penetration levels may have an impact on the distribution system, resulting in voltage unbalance, voltage rise, and reverse power flow, all of which

contribute to higher power loss [11], [12]. This negative impact has an effect on grid operation and control since the low-voltage distribution system is not designed to accept external power sources such as PV devices.

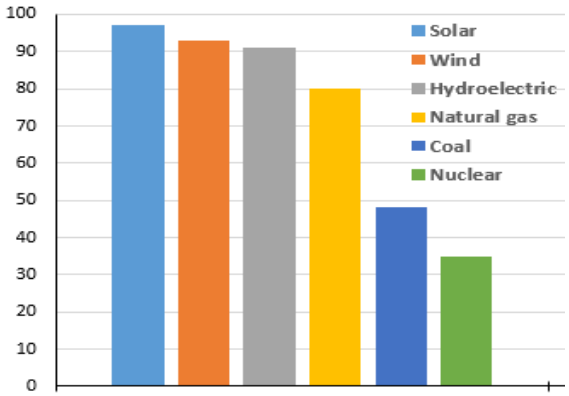

Fig. 1: Public use of renewable energy worldwide, [1]

As PV integration on the distribution network increases, the technical influence needs to be examined and determined. This study investigates the impact of PV system integration on a distribution network using an adapted IEEE 13 bus test system with domestic and industrial feeders and real-time time series analysis of solar irradiance data, [13], [14]. The integration level is adjusted to adequately reflect the effects of PV integrated into the distribution network.

2 Description of Modelled System

Figure 2 depicts the layout of a 10 kW PV system simulated for this study, including all electrical power components and the DC-DC boost converter, which increases the PV voltage at maximum power from 273 Vdc to 500 Vdc. The Incremental Conductance (InCond) MPPT algorithm improves duty cycle switching performance. The MPPT is designed to automatically alter the duty cycle to create the voltage required to track maximum power.

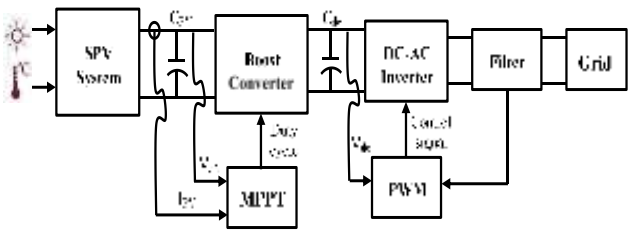

Fig. 2: The basic configuration of the modeled system

A three-phase three-level voltage source inverter (VSI) is connected to the DC-DC converter, which converts the connection voltage of 500 Vdc to 250 Vac. It maintains the system's power factor (PF) at unity. The VSI control system has two feedback loops: an inner loop controls grid currents I_d and I_q (active and reactive components), while an outer loop regulates DC link voltage to ±250V. Equations (1) and (2) explain the voltage equations of a grid-tied inverter in the synchronous reference frame, with L as the filter inductance and R as the filter resistance, [15].

$$V_q = Ri_q + L\frac{di_q}{dt} + \omega Li_d + e_q \quad (1)$$

$$V_d = Ri_d + L\frac{di_d}{dt} + \omega Li_q + e_d \,. \quad (2)$$

where: V_q and V_d are the voltage output of the inverter, I_q and I_d are the inverter currents, ω is the angular frequency of the grid, and e_q and e_d are the grid voltages.

When solar radiation decreases due to cloud movement, the power generated by the PV system follows the Figure 3(a) pattern. In a 10 kW PV system, solar radiation drops from 1000 W/m^2 to 152 W/m^2 at 36°C ambient temperature within 20 seconds of cloud shadow, which reduces the system output from 1700 watts to 139 watts, [16]. Figure 3(b) shows an increase in power after cloud movement, [17]. Most PV systems installed in residential areas operate at a power factor of unity for maximum active power generation; Therefore, in terms of active power, an increase in the PV power capacity corresponds to a decrease in load, [18].

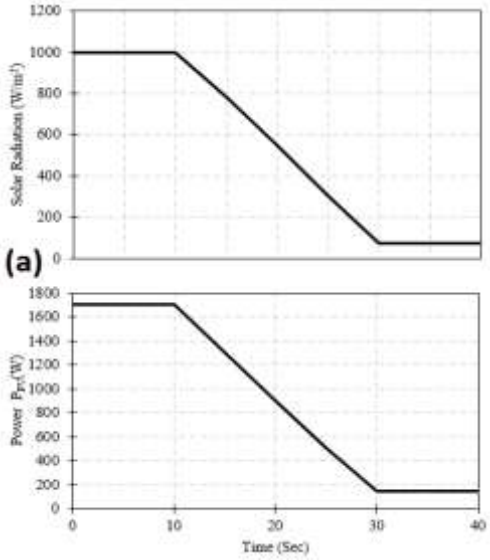

Fig. 3(a): Solar irradiation impact on PV power drop

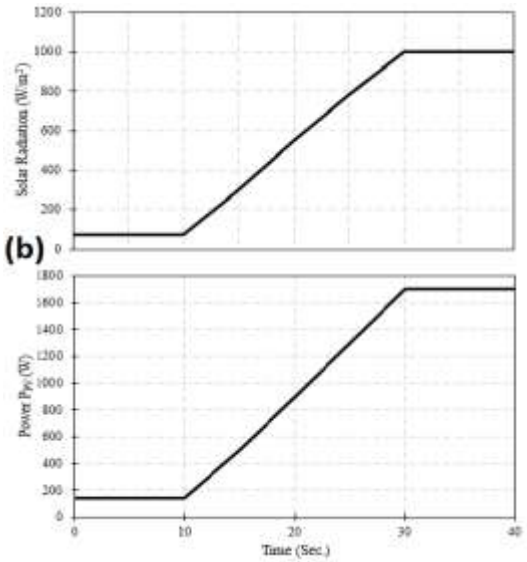

Fig. 3(b): Solar irradiation impact on PV power rise

As solar radiation intensifies, as shown in Figure 3(b), the voltage rises because of the integration of PV systems into the network, which reduces line current and voltage drops along the distribution lines. For significant PV penetration in an unbalanced distribution network, this effect must be thoroughly analyzed. Such impacts may require distribution system operators (DSOs) to implement protective measures to mitigate voltage surges caused by large spikes. While these scenarios are all possible within a distribution network, this study focuses specifically on the widespread adoption of PV systems and the associated challenge of voltage increases they induce.

Grid-integrated PV was simulated using the IEEE 13 bus distribution network. A schematic system diagram can be seen in Figure 4. Buses 632, 633, 634, 671, 692, and 675 are examples of three-phase overhead lines; 645, 646, and 684 are examples of two-phase buses; and 611 and 652 are examples of single-phase buses. With 2.102 MVar and 3.466 MW of distribution loads between industrial and domestic electric power consumers, the distribution system is fairly loaded for a 4.16 kV bus. Along with distributed loads connected in star and delta configurations with constant current and impedance, the network is made up of overhead wires, parallel capacitors, and a grounded delta-star transformer. In line with most modern distribution systems, buses 633 and 634 are linked to a 4point 16 kV/480 V step-down transformer. [19], [20] All buses have a voltage of 4.16 kV, with the exception of bus 634, which has 480 V.

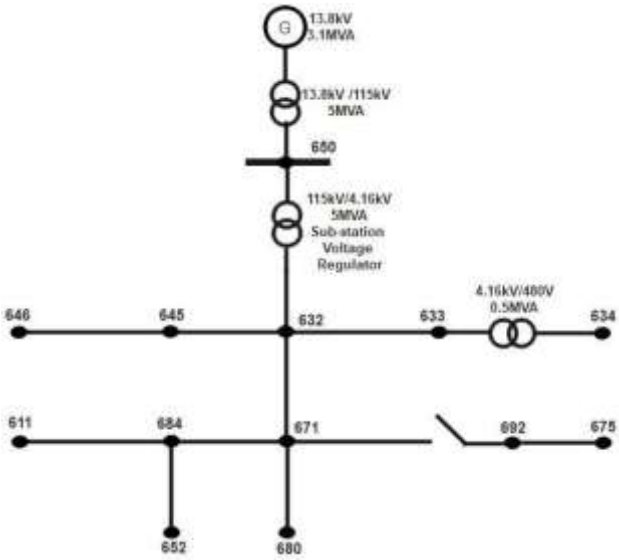

Fig. 4: Schematic of the adapted system

The magnitude of the loads dictated the location of load categories to the busbars, with each bus assigned a certain load category (i.e. residential or commercial). The distribution network's electrical restrictions were analyzed using power flow results, which took into consideration the current across the lines while keeping the voltage within the permitted range (0.95-1.05 p.u), [21]. The iterative equation was used in the power flow analysis to compute the network's power losses, voltage, voltage angles, and active and reactive power.

3 Test System Analysis Approach

Equations (1) through (5) were used to select and design a polycrystalline PV module that would satisfy the needs of the various scenarios in this study. The effects of PV penetration on an unbalanced distribution network were investigated using a MATLAB/Simulink model of an adapted IEEE-13 bus test system. The model file was updated with the network parameters, and the system's baseline results were contrasted with varying PV penetration levels. Grid-integrated PV penetration levels of thirty, forty, and fifty percent of the total load were subsequently put into practice after first creating and testing the model base scenario without PV [22]. Next, the effects of various penetration levels were looked at. The voltage curve and power losses are examined using the snapshot power flow analysis method [23], [24].

3.1 PV Module Model

A single diode circuit was utilized to evaluate the parameters of a single PV cell and compute the output current in Equation (3) [25], [26].

$$I = I_{ph} - I_d \tag{3}$$

where; I_{ph} = photocurrent, I_d = diode current, that is proportionate to the saturation current.

Equations (4) and (5) show that a PV cell's output current is proportional to temperature and solar irradiance.

$$I_{ph} = (I_{SC} + K_i \Delta T)\frac{G}{G_O} \tag{4}$$

Where: I_{ph} = photocurrent; I_{SC} = short-circuit current; K_i = temperature co-efficient of the cell I_{SC}; ΔT = change in cell temperature (K); G = irradiance (kW/m^2); G_O = nominal irradiance (kW/m^2).

The impact of temperature on the saturation current (I_o) of the PV cell is expressed in equation (5) [27], [28].

$$I_O = I_{rs}\left[\frac{T}{T_n}\right]^3 \exp\left[\frac{qxE_g}{nK}\left(\frac{1}{T} - \frac{1}{T_r}\right)\right] \tag{5}$$

The current-voltage characteristic (I-V) can then be described quantitatively, as illustrated in Equation (6).

$$I = I_{ph} - I_O \frac{\left[\exp\left(\frac{qv}{AKT}\right) - 1\right]}{I_d} \tag{6}$$

where: I_{ph} = photocurrent; I_0 = reverse saturation current of the diode; q = electron charge; A = diode ideality constant, K = Boltzmann constant, and I_d = Shockley diode current, [1].

Equation (7) represents the real version of a solar module modified to accommodate the serial/parallel configuration of the PV modules, [29], [30].

$$I = I_{ph} - I_O\left[\exp\left(\frac{I_{ph}R_s}{V_t}\right) - 1\right] - \frac{\left(V_{pv} + I_{pv}R_s\right)}{R_{sh}} \tag{7}$$

where: I = load current; I_{ph} = photocurrent; I_0 = saturation current; V = output voltage; R_s = series resistance; R_{sh} = shunt resistance V_t = thermal voltage.

3.2 PV Location Scenario

For the best tuning of the D-STATCOM PI controller, the dynamic gravity search algorithm (DGSA) is used, which is based on mass interactions and Newton's laws and ensures errors in a finite time span due to its fast convergence functions. Performance is determined by considering the location of the masses that constitute the population in this algorithm. The four characteristics of a mass are its location, its inertial mass, its active mass due to gravity, and its passive mass. Although the mass's position implied a solution, its gravity and inertial masses were related to the fitness function. Gravity forces all of these particles to move toward each other according to Newton's laws. This effect causes heavier masses, which correspond to good solutions, to move slower than lighter masses, which correspond to bad solutions. After the recorded iteration, the global solution and overall fitness of the problem are determined by the optimal fitness and position of the corresponding agent in the search space. The exploitation step of the algorithm in the system is modeled and shown in Figure 4.

The system was simulated with a single PV array of the required size to provide different penetration levels after obtaining a realistic load profile, [31]. As shown in Figure 5, the PV system was installed on bus 611 to assess its effect on the system.

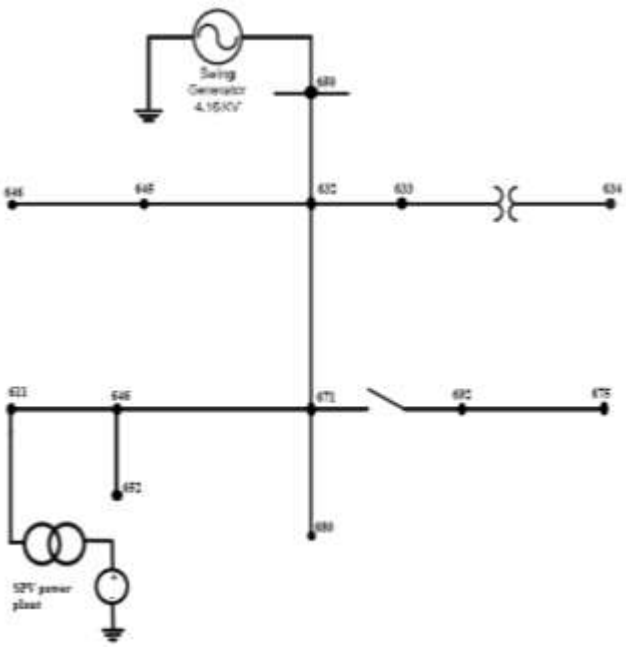

Fig. 5: Illustration of the model in one line

3.3 The Penetration Level of the PV

The maximum output of the PV system divided by the maximum grid consumption - i.e. the total installed loads - defines the PV penetration in this study. In other words, twenty percent of PV integration results in 28 kW power generation at

STC when the maximum grid intake on Phase A of Bus 632 is 150 kW, [32], [33]. The system is believed to produce the most solar energy possible.

$$SPV\ penetration(\%) = \frac{Array\ max.power}{Grid\ max.consumption} \quad (8)$$

A simple iterative power flow analysis was run on each distribution system unit to ascertain the voltage profile, angle, real and imaginary power, and power losses of the test system.

4 Simulation Result

This section discusses the results of various simulation scenarios. Table 1 contains the basic power flow results for the voltage curve and the total active and reactive power with losses, without PV integration into the grid. Normally, the voltage level in the distribution system decreases relative to the main bus of the system due to a voltage drop in the network. Figure 6 shows the voltage diagram for the system without PV integration; The voltage level remains within an acceptable range (0.95 pu to 1.05 pu). The lowest voltage on the network is reported to be 0.9701 on bus 611, and a significant voltage drop is observed on the buses further downstream. Figure 7 provides a detailed examination of the various scenarios in phase A of the network.

Table 1. Base Case power flow results

Description	Solution
Buses	13
Maximum voltage (pu)	1.0559
Minimum voltage (pu)	0.9607
Total active power (kW)	3546.12
Total reactive power (kvar)	1718.65
Total loss on lines and transformer (kW)	112.25
Total loss on lines and transformer (kvar)	315.74

The minimal voltage rises between thirty and forty percent penetration depth, from 0.9599 pu to 0.9793 pu, with a maximal voltage peak of 1.0499 pu, which is under the permitted voltage limit. At fifty percent integration, the voltage rises above the limit, increasing from 1.0499 pu to 1.07621 pu, because power consumer loads are sensitive to voltage swings, this breach may cause damage to them. The grid current also shifts, resulting in a reverse flow of electricity.

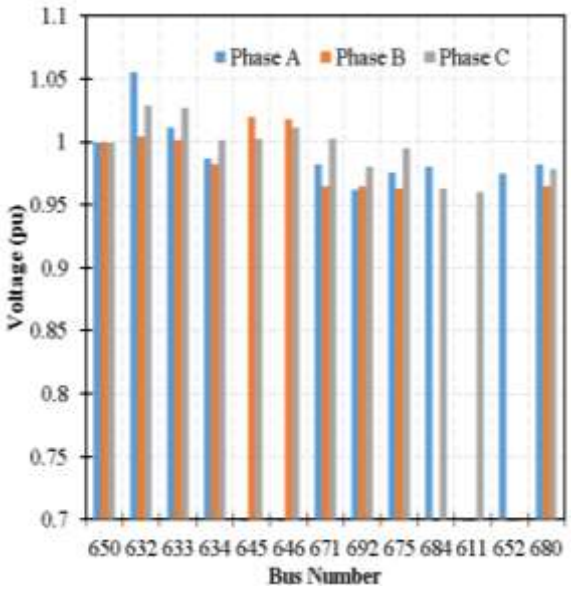

Fig. 6: Voltage magnitude of the base scenario

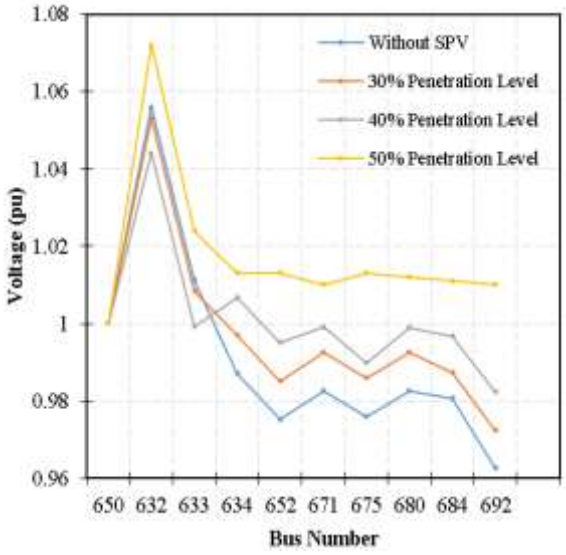

Fig. 7: Different integration scenarios profile on Phase A

Figure 7, Figure 8 and Figure 9 depict the system voltage fluctuation based on a comparative analysis of the results obtained at different PV integration depth on bus 611 in the network.

There was a noticeable voltage drop on the busbar of the grid source prior to the PV generator being installed. The PV system's installation has improved all bus voltages and raised the minimal voltage magnitude from 0.9607 pu to 1.0108 mitigating the trend in Phase A.

On the C phase, the maximum voltage magnitude on bus 632 exceeded the 1.05 pu limit at the fifty percent integration level, indicating that the system voltage stability cannot be maintained at the permissible limit above the forty percent integration level.

Table 2. Overview of System Analysis Findings

System Detail	Base Scenario	30 Percent Scenario	40 Percent Scenario	50 Percent Scenario
Maximal Voltage	1.0559	1.0472 pu	1.0499 pu	1.07621 pu
Minimal Voltage	0.95907 pu	0.9599 pu	0.9793 pu	1.0499 pu to
Active Power Losses	112.245kW	102.82 kW	98.59 kW	130.01 kW
Reactive Power Losses	315.73kVar	317.39 kVar	278.98 kVar	352.64 kVar

Table 2 shows that system losses were drastically reduced with PV integration compared to the results without system integration. Power losses decreased significantly at thirty percent and forty percent PV integration depth, but began to increase at fifty percent penetration, indicating that the grid's PV penetration is limited to fifty percent penetration. This leads to a reverse power flow, which increases power losses in the network.

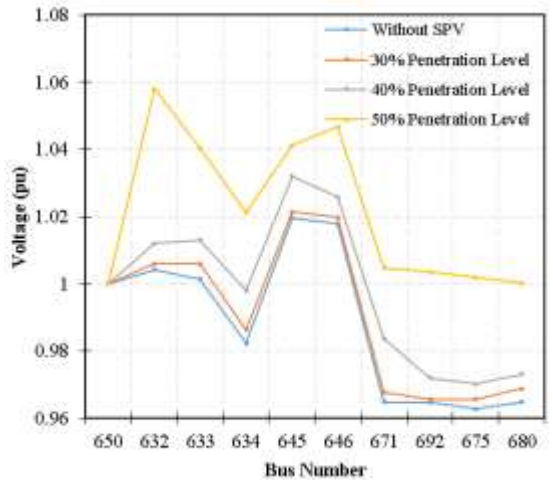

Fig. 8: Different integration scenarios profile on Phase B

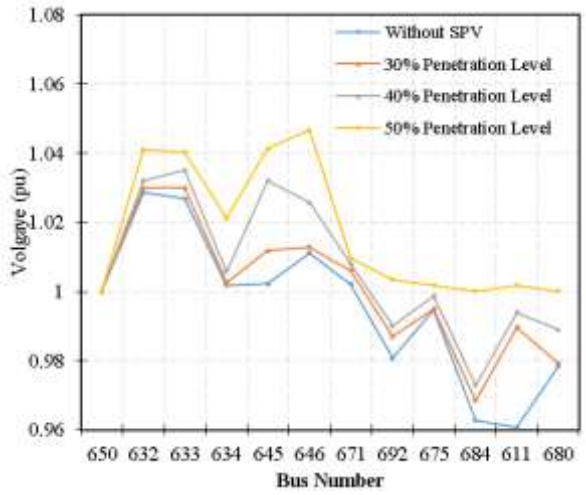

Fig. 9: Different integration scenarios profile on Phase C

5 Conclusion

The influence of integrating PV systems on low voltage distribution systems voltage magnitude and losses in an imbalanced distribution system was studied utilizing an adapted 13 bus test system with a nominal voltage of 4.16 kV/480 V. Four simulated scenarios were considered: the base case study and three different integration levels of the PV system on the grid. The system model and simulation results depict that the PV connection reduces voltage dips on the test system's buses, improves the network voltage profile, and significantly reduces system power losses comparatively to the results obtained without the PV. The highest voltage was determined to be 1.0559 p.u in the base case, which improved to 1.0472 p.u with grid-integrated PV. Similarly, with forty percent PV integration, power losses improve from 315.73 kVar to 278.98 kVar. It has been noted that a forty percent PV integration depth is most acceptable for maintaining a reasonable voltage level and reducing reverse power flow, as a higher integration of the solar system increases power losses on the grid. To avoid power losses, the level of PV integration on the distribution grid should not be too high.

References:

[1] A. Adebiyi, I. Lazarus, A. Saha, and E. Ojo, "Performance analysis of PV panels connected in various orientations under different climate conditions," in *Proceedings of the 5th Southern African Solar Energy Conference (SASEC 2018)*, Durban, South Africa, 2018, pp. 46-51.

[2] S. Mahmoudinezhad, A. Rezania, and L. A. Rosendahl, "Behavior of hybrid concentrated photovoltaic-thermoelectric generator under variable solar radiation," *Energy conversion and management,* vol. 164, pp. 443-452, 2018. https://doi.org/10.1016/j.enconman.2018.03.025.

[3] M. Karimi, H. Mokhlis, K. Naidu, S. Uddin, and A. Bakar, "Photovoltaic penetration issues and impacts in distribution network–A review," *Sustainable Energy Reviews,* vol. 53, pp. 594-605, 2016. https://doi.org/10.1016/j.rser.2015.08.042.

[4] L. Hernández-Callejo, S. Gallardo-Saavedra, and V. Alonso-Gómez, "A review of photovoltaic systems: Design, operation, and maintenance," *Solar Energy,* vol. 188, pp. 426-440, 2019. https://doi.org/10.1016/j.solener.2019.06.017

[5] N. Mansouri, A. Lashab, D. Sera, J. M. Guerrero, and A. Cherif, "Large photovoltaic power plants integration: A review of challenges and solutions," *Energies,* vol. 12, pp. 1-16, 2019 https://doi.org/10.3390/en12193798.

[6] D. Remon, A. M. Cantarellas, J. M. Mauricio, and P. Rodriguez, "Power system stability analysis under increasing penetration of photovoltaic power plants with synchronous power controllers," *IET Renewable Power Generation,* vol. 11, pp. 733-741, 2017. https://doi.org/10.1049/iet-rpg.2016.0904.

[7] F. Katiraei and J. R. Aguero, "Solar PV integration challenges," *IEEE Power Energy Magazine,* vol. 9, pp. 62-71, 2011. https://doi.org/10.1109/MPE.2011.940579.

[8] P. Chaudhary and M. Rizwan, "Voltage regulation mitigation techniques in distribution system with high PV penetration: A review," *Renewable and Sustainable Energy Reviews,* vol. 82, pp. 3279-3287, 2018. https://doi.org/10.1016/j.rser.2017.10.017.

[9] S. K. Solanki, V. Ramachandran, and J. Solanki, "Steady state analysis of high penetration PV on utility distribution feeder," in *PES T&D 2012*, 2012, pp. 1-6 https://doi.org/10.1109/TDC.2012.6281716.

[10] O. S. Nduka and B. C. Pal, "Quantitative evaluation of actual loss reduction benefits of a renewable heavy DG distribution network," *IEEE Transactions on Sustainable Energy,* vol. 9, pp. 1384-1396, 2017. https://doi.org/10.1109/TSTE.2017.2776610.

[11] J. R. Agüero and S. J. Steffel, "Integration challenges of photovoltaic distributed generation on power distribution systems," in *IEEE Power and Energy Society General Meeting*, 2011, pp. 1-6. https://doi.org/10.1109/PES.2011.6039097.

[12] R. Hudson and G. Heilscher, "PV grid integration–system management issues and utility concerns," *Energy Procedia,* vol. 25, pp. 82-92, 2012. https://doi.org/10.1016/j.egypro.2012.07.012.

[13] A. A. Adebiyi, E. E. Ojo, and I. E. Davidson, "Performance Evaluation of a Grid-tied PV System in the East Coast of South Africa," in *IEEE PES/IAS PowerAfrica*, Nairobi, Kenya, 2020, pp. 1-5. https://doi.org/10.1109/PowerAfrica49420.2020.9219905.

[14] A. A. Adebiyi, A. K. Saha, I. J. Lazarus, and E. E. Ojo, "Investigation to Determine the Impacts of PV Penetration on an Unbalanced Distribution Grid," in *IEEE PES/IAS PowerAfrica*, 2019, pp. 116-120. https://doi.org/10.1007/978-981-16-4943-1_40.

[15] Y. Han, X. Fang, P. Yang, C. Wang, L. Xu, and J. M. Guerrero, "Stability analysis of digital-controlled single-phase inverter with synchronous reference frame voltage control," *IEEE Transactions on Power Electronics,* vol. 33, pp. 6333-6350, 2017. https://doi.org/10.1109/TPEL.2017.2746743.

[16] J. P. Ram and N. Rajasekar, "A new global maximum power point tracking technique for solar photovoltaic (PV) system under partial shading conditions (PSC)," *Energy,* vol. 118, pp. 512-525, 2017. https://doi.org/10.1016/j.energy.2016.10.084.

[17] A. Gupta, Y. K. Chauhan, and R. K. Pachauri, "A comparative investigation of maximum power point tracking methods for solar PV system," *Solar energy,* vol. 136, pp. 236-253, 2016. https://doi.org/10.1016/j.solener.2016.07.001

[18] R. Yan and T. K. Saha, "Investigation of voltage variations in unbalanced distribution systems due to high photovoltaic penetrations," in *IEEE Power and Energy Society General Meeting*, 2011, pp. 1-8. https://doi.org/10.1155/2020/4831434.

[19] W. H. Kersting, *Distribution system modeling and analysis*: CRC press, 2006. https://doi.org/10.1201/9781420041736.

[20] A. G. Shaik and O. P. Mahela, "Power quality assessment and event detection in hybrid power system," *Electric power systems research,* vol. 161, pp. 26-44, 2018. https://doi.org/10.1016/j.epsr.2018.03.026.

[21] L. Yu, D. Czarkowski, and F. De León, "Optimal distributed voltage regulation for secondary networks with DGs," *IEEE*

Transactions on Smart Grid, vol. 3, pp. 959-967, 2012. https://doi.org/10.1109/TSG.2012.2190308.

[22] N. Srisaen and A. Sangswang, "Effects of PV grid-connected system location on a distribution system," in *IEEE Asia Pacific Conference on Circuits and Systems (APCCAS 2006) 2006*, 2006, pp. 852-855. https://doi.org/10.1109/APCCAS.2006.342175.

[23] Y. Liu, N. Zhang, Y. Wang, J. Yang, and C. Kang, "Data-driven power flow linearization: A regression approach," *IEEE Transactions on Smart Grid*, vol. 10, pp. 2569-2580, 2018. https://doi.org/10.1109/TSG.2018.2805169.

[24] Z. Wang, B. Cui, and J. Wang, "A necessary condition for power flow insolvability in power distribution systems with distributed generators," *IEEE Transactions on Power Systems*, vol. 32, pp. 1440-1450, 2016.

[25] A. Ayang, R. Wamkeue, M. Ouhrouche, N. Djongyang, N. E. Salomé, J. K. Pombe, *et al.*, "Maximum likelihood parameters estimation of single-diode model of photovoltaic generator," *Renewable energy*, vol. 130, pp. 111-121, 2019. https://doi.org/10.1016/j.ifacol.2024.05.064.

[26] S. Bana and R. Saini, "A mathematical modeling framework to evaluate the performance of single diode and double diode based PV systems," *Energy Reports*, vol. 2, pp. 171-187, 2016. https://doi.org/10.1016/j.egyr.2016.06.004.

[27] X. H. Nguyen and M. P. Nguyen, "Mathematical modeling of photovoltaic cell/module/arrays with tags in Matlab/Simulink," *Environmental Systems Research*, vol. 4, pp. 4-24, 2015. https://doi.org/10.1186/s40068-015-0047-9.

[28] Y. Chaibi, A. Allouhi, M. Malvoni, M. Salhi, and R. Saadani, "Solar irradiance and temperature influence on the photovoltaic cell equivalent-circuit models," *Solar Energy*, vol. 188, pp. 1102-1110, 2019. https://doi.org/10.1016/j.solener.2019.07.005

[29] T. Salmi, M. Bouzguenda, A. Gastli, and A. Masmoudi, "Matlab/simulink based modeling of photovoltaic cell," *International journal of renewable energy research*, vol. 2, pp. 213-218, 2012. https://doi.org/10.20508/ijrer.v2i2.157.g106.

[30] M. A. Hasan and S. K. Parida, "An overview of solar photovoltaic panel modeling based on analytical and experimental viewpoint," *Renewable and Sustainable Energy Reviews*, vol. 60, pp. 75-83, 2016. https://doi.org/10.1016/j.rser.2016.01.087

[31] M. Shaaban and J. Petinrin, "Sizing and siting of distributed generation in distribution systems for voltage improvement and loss reduction," *International Journal of Smart Grid Clean Energy*, vol. 2, pp. 350-356, 2013. https://doi.org/10.12720/sgce.2.3.350-356.

[32] R. A. Kordkheili, B. Bak-Jensen, R. Jayakrishnan, and P. Mahat, "Determining maximum photovoltaic penetration in a distribution grid considering grid operation limits," in *2014 IEEE PES General Meeting| Conference & Exposition*, 2014, pp. 1-5. https://doi.org/10.1109/TSTE.2012.2225115.

[33] C. Gaunt, E. Namanya, and R. Herman, "Voltage modelling of LV feeders with dispersed generation: Limits of penetration of randomly connected photovoltaic generation," *Electric Power Systems Research*, vol. 143, pp. 1-6, 2017. https://doi.org/10.1109/ACCESS.2017.2747086.

[34] M. M. Begovic, I. Kim, D. Novosel, J. R. Aguero, and A. Rohatgi, "Integration of photovoltaic distributed generation in the power distribution grid," in *45th Hawaii International Conference on System Sciences*, 2012, pp. 1977-1986. https://doi.org/10.1109/HICSS.2012.335.

[35] D. Iioka, T. Fujii, D. Orihara, T. Tanaka, T. Harimoto, A. Shimada, *et al.*, "Voltage reduction due to reverse power flow in distribution feeder with photovoltaic system," *International Journal of Electrical Power & Energy Systems*, vol. 113, pp. 411-418, 2019. https://doi.org/10.1016/j.ijepes.2019.05.059.

Contribution of Individual Authors to the Creation of a Scientific Article (Ghostwriting Policy)

The authors made equal and substantial contributions to this research, participating in all stages, from defining the research context to the conclusion.

Sources of Funding for Research Presented in a Scientific Article or Scientific Article Itself

I want to use this opportunity to appreciate Tshwane University of Technology for the success of this research work.

Conflict of Interest

The authors have no conflicts of interest to declare.